

Article

Novel Combined Approach of GIS and Electrical Tomography to Identify Marsh/Lake at Kastrouli Late Mycenaean Settlement (Desfina, Greece)

Ioannis Liritzis ^{1,2,3,4,*}, Niki Evelpidou ⁵, Ilias Fikos ⁶, Alexandros Stambolidis ⁶, Nectaria Diamanti ⁶, Theano Roussari ⁶, Maria Tzouxanioti ⁴, Prodromos Louvaris ⁶ and Gregorios N. Tsokas ⁶

¹ Laboratory of Yellow River Cultural Heritage, Key Research Institute of Yellow River Civilization and Sustainable Development, Henan University, Minglun Road 85, Kaifeng 475001, China

² Collaborative Innovation Center on Yellow River Civilization, Henan University, Minglun Road 85, Kaifeng 475001, China

³ European Academy of Sciences & Arts, St. Peter-Bezirk 10, A-5020 Salzburg, Austria

⁴ Department of Archaeology, School of History, Classics and Archaeology, College of Arts, Humanities & Social Sciences, Edinburgh University, Edinburgh EH8 9AG, UK

⁵ Faculty of Geology and Geoenvironment, National and Kapodistrian University of Athens, Panepistimioupolis, Zografou, 157 84 Athens, Greece; evelpidou@geol.uoa.gr (N.E.); mtzouxanioti@geol.uoa.gr (M.T.)

⁶ Exploration Geophysics Laboratory, Department of Geology, Division of Geophysics, Aristotle University of Thessaloniki, 541 24 Thessaloniki, Greece; ifikos@geo.auth.gr (I.F.); astamp@geo.auth.gr (A.S.); ndiamant@geo.auth.gr (N.D.); roussaria@geo.auth.gr (T.R.); info@geo.auth.gr (P.L.); gtsokas@geo.auth.gr (G.N.T.)

* Correspondence: liritzis@henu.edu.cn

Citation: Liritzis, I.; Fikos, E.; Stambolidis, A.; Diamanti, N.; Roussari, T.; Tzouxanioti, M.; Louvaris, P.; Tsokas, G.N. Novel Combined Approach of GIS and Electrical Tomography to Identify Marsh/Lake at Kastrouli Late Mycenaean Settlement (Desfina, Greece). *Quaternary* **2022**, *5*, 26. <https://doi.org/10.3390/quat5020026>

Academic Editor: José Javier Baena Preysler

Received: 4 April 2022

Accepted: 29 April 2022

Published: 4 May 2022

Publisher's Note: MDPI stays neutral with regard to jurisdictional claims in published maps and institutional affiliations.



Copyright: © 2022 by the authors. Licensee MDPI, Basel, Switzerland. This article is an open access article distributed under the terms and conditions of the Creative Commons Attribution (CC BY) license (<https://creativecommons.org/licenses/by/4.0/>).

1. Introduction

Landscapes are constantly changing as a result of climatic impact; the formation of streams and rivers; and variations in riversides, flooding, water erosion, and tectonic causes. Combining archaeology with investigations of ancient marshes or pods/lakes is figurative for the resetting of palaeoenvironmental status and our comprehension of anthropic landscape impacts. Studying relict lakes from soils and applying surface geomorphology to geoarchaeological datable surfaces (pedoarchaeology) are distinctly helpful in this process, as well as in establishing a chronology of pedogenesis and dwellings [1].

Settlements in Greece were set on high hills to protect against occasional flooding. However, during the prehistoric eras, settlements were placed near lake-margin marshes and ponds. The abundance of aquatic resources in the lake margin and its vulnerability to short- and long-term fluctuations have had an impact on both subsistence and settlements and are thought to have motivated a para-agricultural economy [2]. In Greece, throughout its long history, water has played an indispensable role in the life of these ancient societies, and Greeks were rigorous in the field of water management, carrying out an impressive variety of hydraulic works [3,4]. Hence, the first lakes may have developed into swamps/marshes, introducing malaria from insects (malaria is caused by parasites such as the plasmodium, and it is transmitted to humans by mosquitoes) and hindering agriculture and livestock; thus, attempts to dry out the lakes may have been made [5,6]. In addition, these waterbodies have records of long environmental variation changes and human resource use, as well as nurturing high rates of endemism and biodiversity, with the freshwater enhancing algae overgrowth, fed by excess nutrients [7].

The presence of an ancient lake and/or marsh can be confirmed using various methodological tools: borehole logging [8], archaeological witness [9], historical accounts, mythological legends (see lake gods), and electrical tomography [10] have been quoted.

The drainage of water from agricultural land has existed for a long time in history, dating back to the earliest civilizations in the Middle East since about (circa, ca.) the fourth millennium before our common era (BCE). In the southeastern Mediterranean, the Minoan and Mycenaean cultures devised techniques and master plans for the drainage of agricultural lands in the ca. 15th century (c.) BCE. Since the decline and fall of the Aegean-Anatolia region and Near and Middle East civilizations, society retrieval and agricultural innovation during the Archaic and Classical periods (ca. 9th–4th c. BCE) encompassed successful hydraulic endeavors, mastering drainage and irrigation techniques. Moreover, Mesoamerica, India, and China have extensive histories of drainage and examples of underground cisterns since prehistoric times and such evidence has been found elsewhere in Greece, e.g., in Mycenae, Athens, Tyrins, Zakros, and Tylissos [11–14]. Earlier engineering works are evident at Lake Kopais, Boeotia, where Late Mycenaeans from Orchomenos, Gla, or Thebes settlements drained the lake [6], as indicated by a GIS-based survey of archaeological datasets [15].

In the present paper, the plain adjacent to the Kastrouli fortified settlement (Desfina village, near the town of Delphi, Phocis province, Central Greece) is investigated concerning drainage activities using a geoarchaeological approach (Figure 1). It is a wetland agrarian area, with the presence of a Late Mycenaean site from 14th c. BCE., which was also inhabited at later times. The site has been systematically excavated since 2016, and an interdisciplinary methodological approach has been developed. Chronological studies using radiocarbon (^{14}C) and luminescence dating, characterization and provenance, geophysical prospection investigations, and coastal geoarchaeology have produced invaluable results regarding the Mycenaean presence in southern Phocis [16–23].

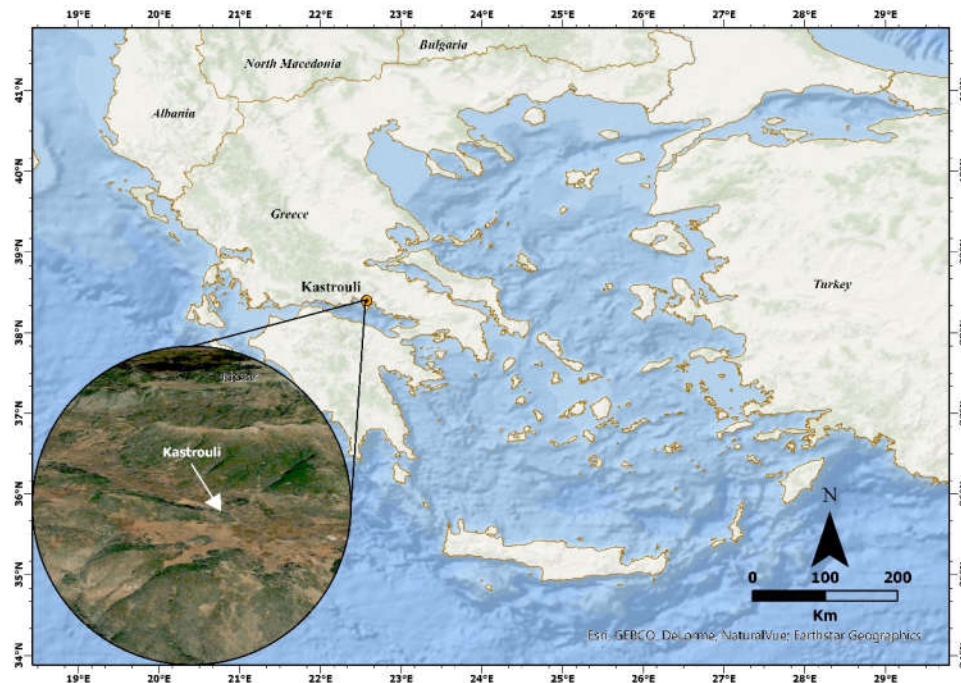


Figure 1. Aerial view of the Kastrouli settlement and environs and the location of the site in the eastern Mediterranean. The traced, shaded landmark on the edge of the plain is noticeable, and it is where water gathers during the winter; this geometric mark indicates plant debris forming a traced boundary of a littoral zone similar to shorelines.

Here, we advance these investigations in the search for the presence of an ancient lake or marsh/swamp by first following a novel approach combining a geographical information system (GIS) with a digital elevation model (DEM) and thematic maps, focusing on the sloping of the terrain, together with electrical resistivity tomography (ERT) traverses, supported by apparent archaeological remains.

The prompts for this investigation were the contemporary sporadically flooded plain at the Meteles plain off the Kastrouli hillock during winter and the presence of two sinks built with a rim and an entrance leading via a channel to a natural underground fissure. The surface ruins of the two built sinks were apparently engineered to lead seepage water into a natural aquifer present in the limestone bedrock; this observation led to an earlier report on the alleged ancient hydraulic works in the area [22]. These two features suggest the possible existence of a marsh/small lake in the past, as they indicate earlier attempts to drain the formed small lake/marsh. The natural sinks were probably first recognized by the ancient habitants of the area in the nearby prehistoric Kastrouli settlement or its occupants at later times. Thus, the natural outpour was engineered to facilitate drainage. Today, the plains around Desfina village are inundated with long-lasting rainfall during the winter (Figure 2).

Here, we present the first phase of a GIS and electrical tomography combined novel approach to examine the presence of an old swamp/marsh or small lake to confirm the hydraulic works at Kastrouli being an attempt to drain the plain in the past.



Figure 2. A panoramic photo of formation of a seasonal lake in the vicinity of Desfina (on the right), and snowy Mount Parnassus can be seen in the background (© IL).

The objective of the present paper is to identify and define the boundaries of an ancient marsh/lake using a novel combined approach of a digital elevation model, GIS, and electrical tomography in light of the remains of built surface works, made to reroute vast amounts of flood release into two sinkholes.

2. Methods and Instrumentation

2.1. Electrical Resistivity Tomography (ERT)

Electrical resistivity tomography (ERT) is a sophisticated geophysical method that determines the Earth's subsurface resistivity by generally taking measurements on the ground surface [24]. ERT data are rapidly collected on profiles and provide a cross-sectional (2D) plot of the so-called apparent resistivity ($\Omega \cdot m$) versus depth. This is a technical quantity, which is a function of the true resistivities of the formations, constituting the subsurface setting. Next, these data are inverted to yield the distribution of the true resistivity in the subsurface, which is called "electrical resistivity tomography". ERT interpretation is a straightforward task and leads to accurate representations of the geometry and lithology of the subsurface geologic formations.

Clay, metallic oxides, and sulfides are common sedimentary materials that can conduct electrical currents through the material itself. As such, the specific resistance of most near-surface sedimentary materials is indicative of the quantity and chemistry of the pore fluids within the material. The range of resistivity responses for one specific formation depends on the saturation level, ion concentration, the presence of organic fluids (such as non-aqueous-phase liquids), the temperature, the pressure, and the porosity [25,26]. The general principles that ERT is based on are what have been in use by geophysicists for almost a century [27]. Recent developments in field equipment and data processing techniques have enabled rapid two-dimensional routine research and three-dimensional research. Older one-dimensional resistance surveys are still common and useful in many cases but have problems interpreting areas of complex 2D or 3D geology.

Designing the exact parameters of our ERT survey in advance was not possible, mainly due to the lack of information regarding the maximum depth of investigation required. However, since the estimated maximum depth of investigation was of the order of several tens of meters, we employed two custom-built 24-channel cables with 11 m maximum electrode separation. This way, we could modify the spacing and the total length of each ERT from a few meters up to more than 500 m, thus modifying the maximum depth of the investigation and resolution accordingly (Figure 3).



Figure 3. On the site of Meteles plain arranging ERT measurements (© IL). Upper left: four of the co-authors preparing for the ERT measurements in situ, Left: two co-authors lay the cables for ERT, Right: taking a reading in situ.

Apart from the 2 cables, we used the IRIS Syscal Pro, 10—channel system together with 48 steel electrodes. The positioning of each line was determined with differential GPS, ensuring accuracy of a few centimeters.

The first ERT1 was measured with electrode spacing $a = 6$ m, providing a total length of 282 m and a maximum depth of investigation greater than 60 m. Based on the preliminary results of ERT1, we implemented greater electrode spacing in the second ERT2. Hence, we exploited the maximum possible separation $a = 11$ m, reaching a maximum depth of investigation of almost 100 m and a total length of 517 m (Figure 4).

The calculation of the true resistivity distribution was performed with the use of DC_2DPro [28], an iterative inversion algorithm that transforms the arrangement of the resistivity data into a geology model that yields the observed distribution of the resistivity values.

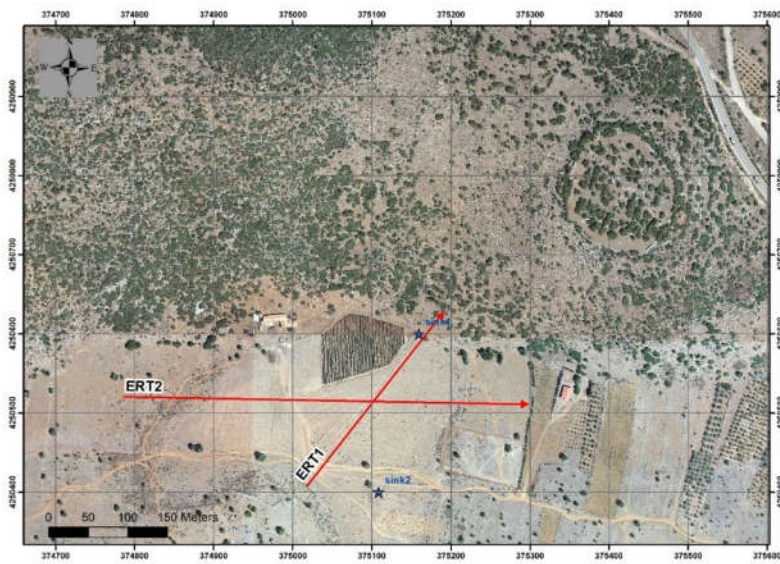


Figure 4. Aerial view of Kastrouli (round circle) and environment with the two ERT traverses (in red). The two sinkholes sink1, sink2 are shown in blue stars. The traced, shaded landmark on the edge of the plain is noticeable, and it is where water gathers during the winter; this geometric mark indicates plant debris forming a traced boundary of a littoral zone. Axis numbers are the HGS (Hellenic Geodetic System) 1987 coordinates in meters.

2.2. GIS, DEM, and Thematic Maps

Geomorphological observations in the Meteles area were made in the field, from existing maps, and from aerial photos derived from an Unmanned Aerial Vehicle (UAV) (DJI Mavic Mini). For the accuracy of field data collection, RTK-GNSS equipment (SPEC-TRA SP-80) was used. All data were stored in a geographic information system in order to develop a geodatabase for further analysis. Topographic data were simulated in order to produce a digital elevation model (DEM). Based on DEM, a geographical distribution of morphological slopes was developed [29,30], as well as of the drainage system and drainage basins. Analysis of the morphological slopes using several thematic maps helped to investigate, describe, and analyze the changes in the relief.

3. Results

3.1. ERT

Electrical tomography was applied, deploying two traverses along and across the plain (Figure 4). The low conductivity, due to the extremely dry ground during summer (Figure 5), resulted in very high contact resistances, which were compensated for by watering the electrodes. The yielded resistivity imaging of the subsurface indicates a limestone bedrock whose ceiling undulates. At its shallower parts, its depth varies between 0 and 7 m, whereas its depth is ca. 60 m at its deeper parts. The bedrock depth extends beyond 90 m. Figure 6 displays two electrical tomographies. They show variable underground topography with loose sedimentary deposits near the surface (5–10 m). Figure 7 shows a “fence diagram” of the two electrical tomographies. The two sinkholes passing through the natural fissures of the low-resistance limestone bedrock are noticeable. A depression filled with sediments is found along ERT1 at a depth of ca. 60 m, with a locus of loose sediment at 30–40 m of very low resistivity (10–20 ohm·m). The two sinkholes in ERT1 are connected to channels through loose resistance, leading to discharge through the hard rock. In recent times, discharge occurs via natural dryness, but in ancient times, hydraulic works were necessary to remove the water. Since these two engineered

sinkholes lie on the present surface, this implies that the boundary of an ancient marsh or small lake could have been close to these sinkholes, while hydraulic drainage works should have been made when the water level was within a meter or less from the present ground surface. The latter delineates the maximum extension of the marsh/lake.



Figure 5. Characteristic crevices and cracks are formed in the ground due to summer dryness (© IL).

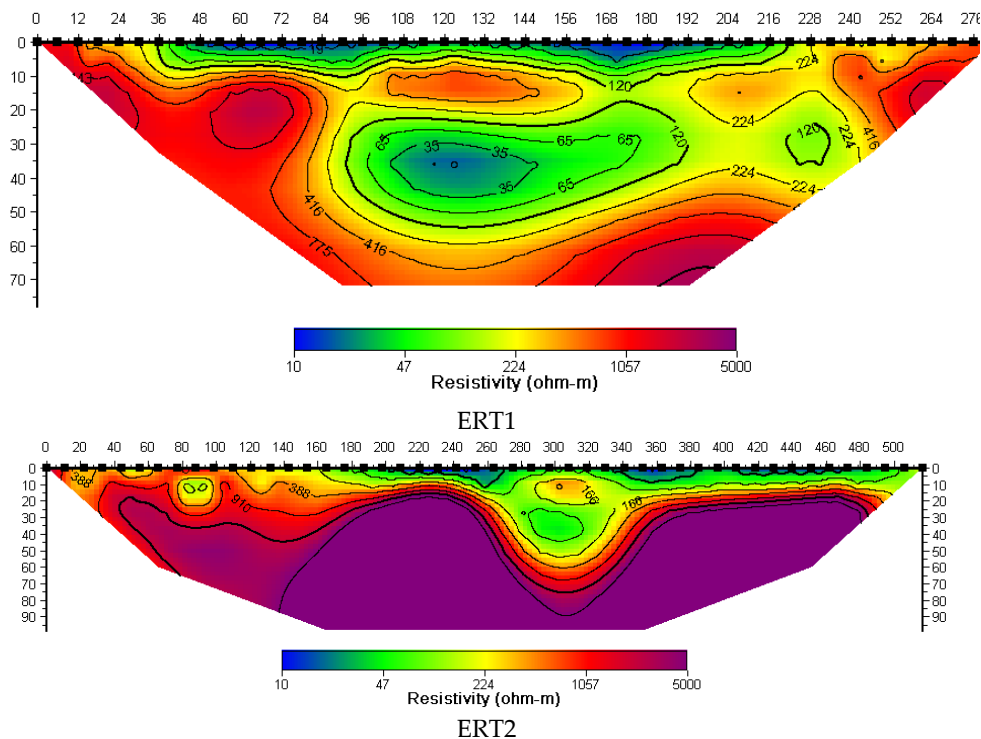


Figure 6. Electrical resistivity tomographies along the profiles ERT1 and ERT2.

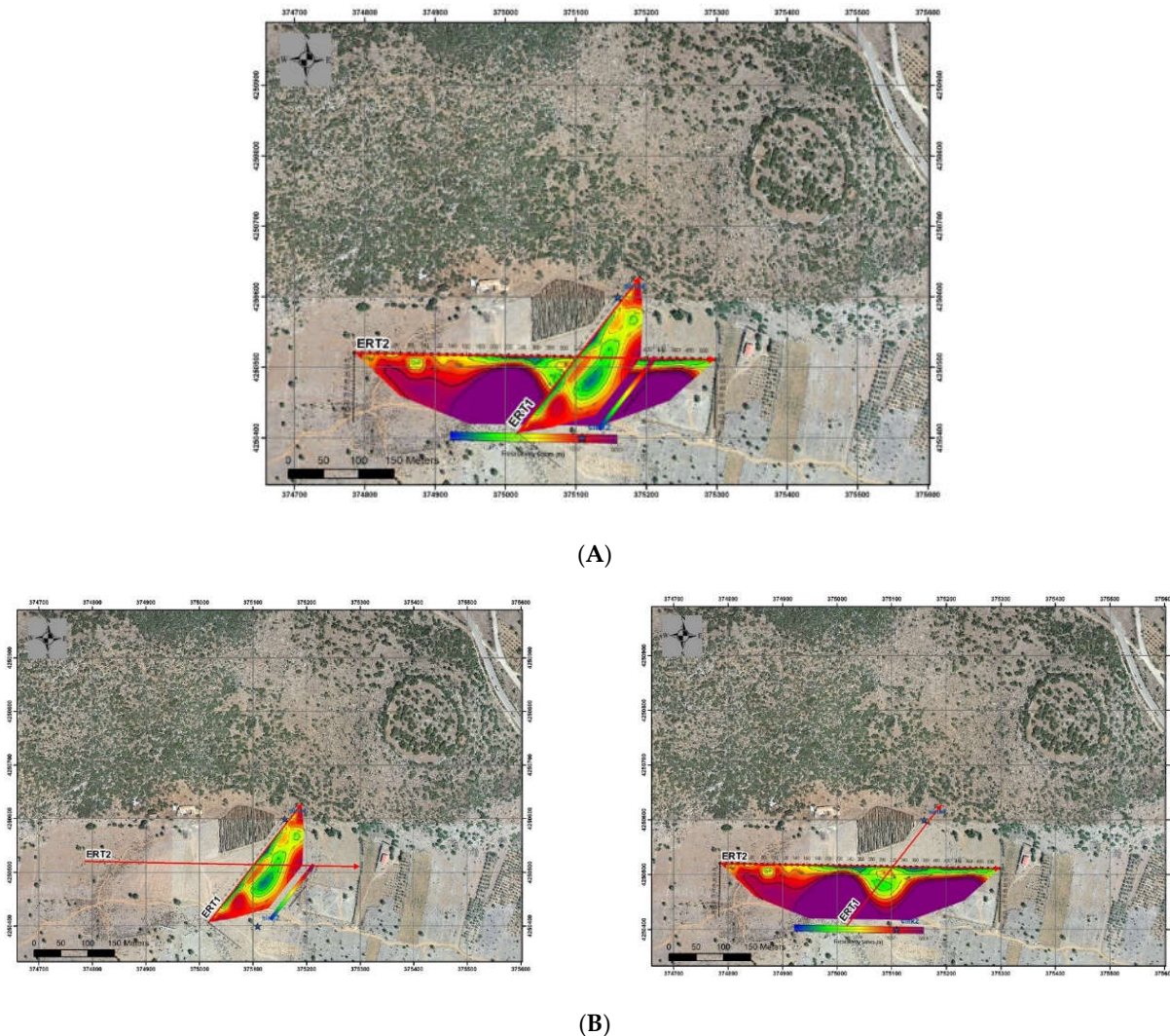


Figure 7. (A) Fence diagram of the electrical topographies (ERT1 and ERT2) and (B) the ERTs of the Meteles basin shown such that their relation to the basin becomes apparent. Axis numbers are the HGS (Hellenic Geodetic System) 1987 coordinates in meters.

3.2. Slopping via Thematic Maps, GIS, and DEM

It is evident that, nowadays, the geomorphological characteristics of the area of Meteles are not the same as those 3200 years ago. The large amounts of sediment transported during this period must have changed the bottom of a small lake.

For this purpose, using ArcGIS Pro v. 2.9.2. software, we set up a high-resolution DEM 5×5 m, which was derived from topographic maps at a scale of 1:5000, spatial data produced from a UAV survey in the main study area [31], and RTK-GNSS data (Figure 8). In the present study, the UAV data provide an accurate metric documentation of the wider archaeological site.

The DEM was created in order to identify changes in the relief and in the physical characteristics of the study area, e.g., surface drainage information, such as hydrographic network and drainage basins, and to calculate the morphological slopes. The map of the morphological slopes depicts the geographical distribution of the morphological slopes within the drainage basins and, at the same time, reveals where the surface morphology could indicate the existence of sinkholes.

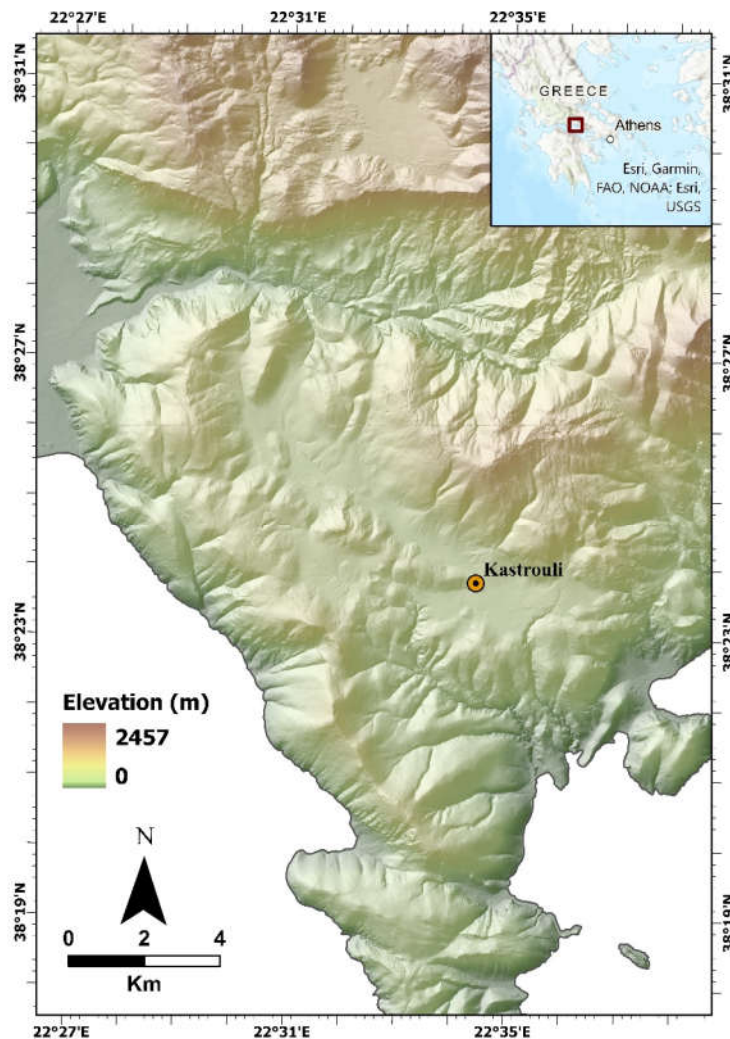


Figure 8. Digital elevation model of Southern Phocis area with Kastrouli fortified settlement.

Based on the Food and Agriculture Organization of the United Nations (FAO) slope classification, the analysis indicates a relatively low slope area or flat-to-sloping area of 3.04 Km² near the Kastrouli fortified settlement (Figure 9), with inclinations fluctuating between 0 and 5 degrees or 0 and 8.75% (Figure 10). In this area, the authors identified two depressions in the ground, called sinkholes, which are indications of unnatural external surface drainage. Based on the study conducted by Ford and Williams [32,33], sinkholes are produced from different geological processes of endogenous and exogenous origin. Moreover, these sinkholes are located in the relatively low slope area (Figures 10 and 11), which consists mainly of alluvial deposits, limestone formations, and second-generation bauxite ore deposits, indicating both depression and subsidence. Figures 10–12 illustrate variations in the morphological slopes, and the morphological slopes of 1°, 2°, and 3° are delineated to illustrate the area where sinkholes developed.

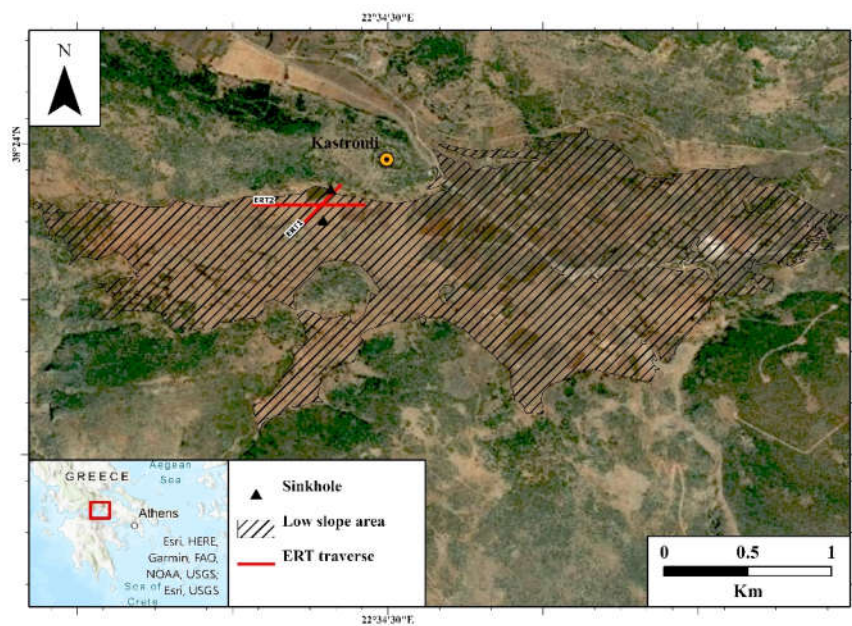


Figure 9. The (northeast) map, derived from the high-resolution digital elevation model, showing the position of the sinkholes, the two ERT traverses (red) and the relatively low slope area.

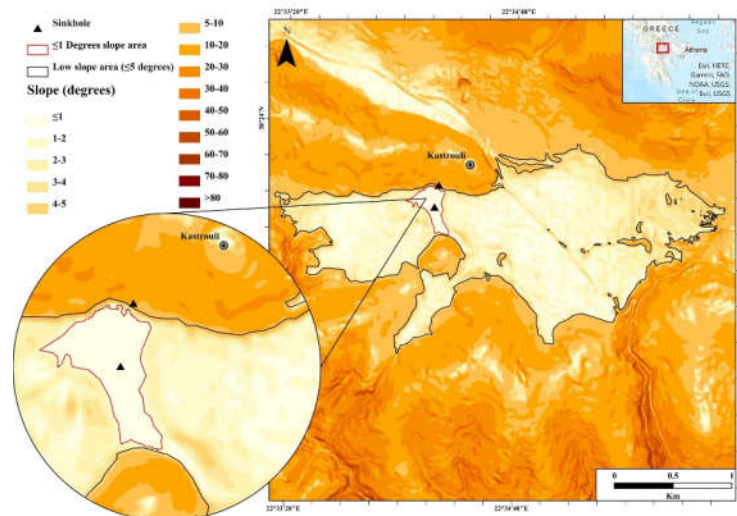


Figure 10. Morphological slopes of Kastrouli area. The black outline identifies the area with inclinations fluctuating between 0 and 5 degrees (0 and 8.75%). On the contrary, the red outline indicates an area of 0.06 Km², with inclinations fluctuating between 0 and 1 degrees (0 and 1.75%). Gray triangles are the sinkholes.

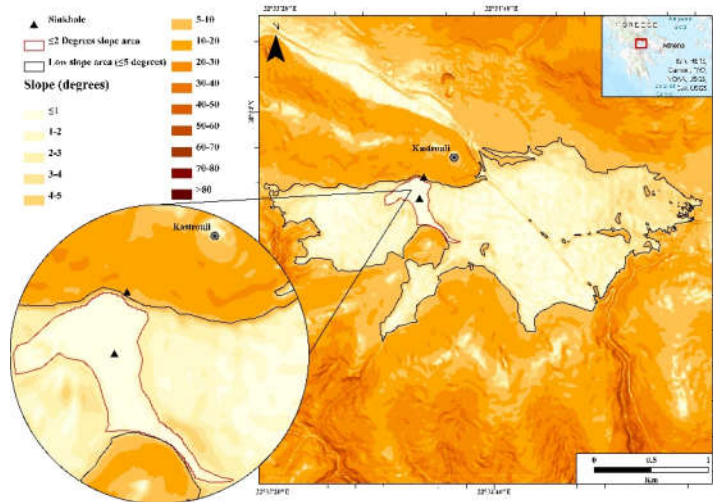


Figure 11. Morphological slopes of Kastrouli area. The black outline identifies the area with inclinations fluctuating between 0 and 5 degrees (0 and 8.75%). On the contrary, the red outline indicates an area of 0.10 Km², with inclinations fluctuating between 0 and 2 degrees (0 and 3.49%). Gray triangles are the sinkholes.

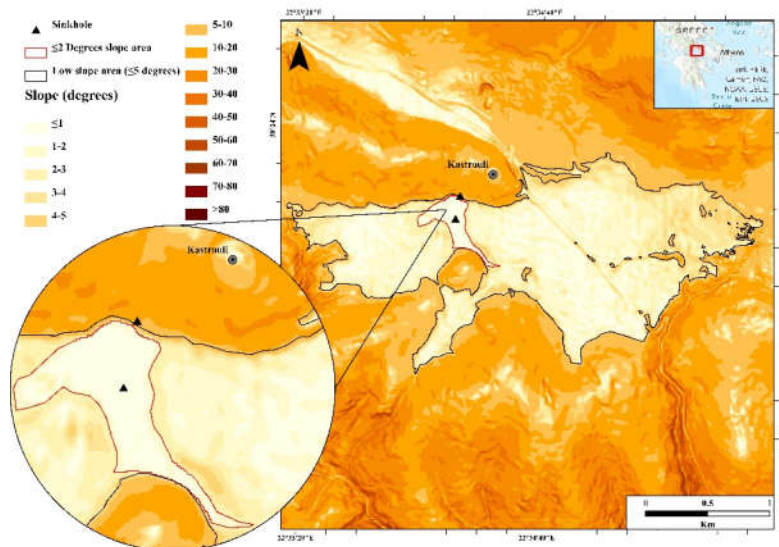


Figure 12. Morphological slopes of Kastrouli area. The black outline identifies the area with inclinations fluctuating between 0 and 5 degrees (0 and 8.75%). On the contrary, the wide red outline indicates an area of 2.33 Km², with inclinations fluctuating between 0 and 3 degrees (0 and 5.24%). Gray triangles are the sinkholes.

4. Discussion

The broader geological area of Kastrouli–Desfina consists mostly of Alpine formations of the Parnassus–Ghiona zone and is partly covered by Neogene–Quaternary terrestrial loose deposits. South of Kastrouli, at the coastal zone, there is a small outcrop of the Pindos zone. This Parnassus–Ghiona mountain zone consists of a limestone sequence with bauxite intercalations. The limestones are neritic, middle-to-thick layers of the Triassic to Cretaceous and are covered by flysch, which includes brown-red siltstones, mudstones, and sandstones.

The upper Cretaceous limestones vary in thickness between 150 and 200 m. The basins around Kastrouli and the Desfina valley are filled with Quaternary, mainly Holocene sediments [19,34,35].

At the edges of the Kastrouli–Meteles basin, man-made structural activities on a natural crevice in the bedrock have formed two constructed sinkholes. The southern one has a western opening of around 1.40 m and a width of 0.60 m, and around twelve descending stairs leading to an underground tunnel intentionally dug to divert flood water, reaching a ca. 4 m chamber (Figure 13). To date, no extensive survey has been conducted regarding the ceramic sherds present at the bottom of the tunnel and/or the dating of the stone construction with its mortar. Thus, any dating is possible from the Late Bronze to the medieval period and maybe even modern times.



Figure 13. The southern sinkhole in the center of Meteles plain valley. From the present surface, the top of the interior with steps. Photos are taken from various angles of same sinkhole 2 (© IL).

The second one, north of the plain at the bottom of the foot slope of Kastrouli hill (Figure 14) and built with medium-sized stones, includes a cistern of about 5 by 3 m with a drainage sink, and the drainage location is covered by sediments. This sink was of particular importance, as it has a small-sized arched bridge made with stone block and unpolished stones with mortar, and it is of a larger construction and an obviously engineered channel to drain the water.



Figure 14. The cistern of the northern side sinkhole at Meteles, close up (left) and at a distance (right) (© IL).

The waters draining into this initially deep basin, made up of variable thicknesses of sedimentary deposits, as shown by ERT, carry with them much of the suspended sediment that has been transported to date by the presence of rivers and streams from the local catchment area. The actions of the current and the waves along the shore of the swamp/small lake are responsible for the additional erosion and sediment deposition, and some material may have been introduced as a result of the action of the wind; furthermore, hydraulic effects dominate in small lakes. Seasonal rivers and streams in the environment transport material of many different sizes, mainly of fine-to-medium grain size, the largest being rolled along torrents. River water enters the Meteles basin during Holocene, and the bed-load transport of the impermeable rock ceases upon reaching today's flat area. The lake basin water outlets seem to define the boundary limits adjacent to the outflow. Because the dynamic processes that keep materials suspended are generally more active near the water inlet to the formed swamp, sediments are usually sorted by size. Rocks, pebbles, and coarse sand are located near the shore, while the finer sand, mud, and silt are, in most cases, in the center of the basin (borehole log work in progress).

Both man-made structures have a cistern, a dug pipe similar to a channel to direct the gathered waters into the openings of the two sinkholes. Drainage was probably made to protect the cultivated land and to avoid a swamp associated with health problems, as it is situated precisely ahead of the district. These are excellent reasons to conclude that the current drainage works in the Meteles plane are later restorations or modifications of a system designed by the Mycenaean residents of the fortified village of Kastrouli [22].

Both ERT measurements, with total lengths of 282 and 517 m, showed that there is indeed a dip in the investigated area with an irregular topography filled with Quaternary sediments at depths ranging between 5–6 m and 60 m for ERT1 and 100 m for ERT2.

However, the high-resolution DEM using ArcGIS derived from topographic maps at a scale of 1:5000, UAV, and RTK-GNSS data identified morphological slopes and other interesting physical characteristics.

This analysis indicated a relatively low slope area of around 3 Km², with inclinations fluctuating between 0 and 5 degrees (0 and 8.75%) and sinkholes produced from different geological processes of endogenous and exogenous origin. Depression and subsidence are observed, filled in with alluvial deposits, limestone formations, and second-generation bauxite ore deposits. It is of interest to note that the area covered by the slope of less than

1 degree ($\leq 1.75\%$) is 0.61 Km^2 ($\sim 240 \times 240 \text{ m}$), with two natural outcrop barriers, one being the Kastrouli foothill and the other being close to the southern sink. The increase in the area is profound for slopes higher than 3–5 degrees (5.24–8.75%).

The piedmont in the investigated area gradually increases in elevation at the base of Kastrouli hill in the present upland area. The transition zone between the Meteles plain and the low-relief adjacent hillocks are well defined in the thematic slope maps reinforced by ERT. The traced area between 0 and 5 degrees (0 and 8.75%) results in a dissected plateau of the Desfina landscape and consists of alluvial fans and coalesced alluvial fans supported by the torrent and stream GIS mapping of the region (Figure 15). An area of 2.33 Km^2 makes it a large region, which, in the past, may have suffered from flooding, with dimensions of 3 Km by 1–2 Km.

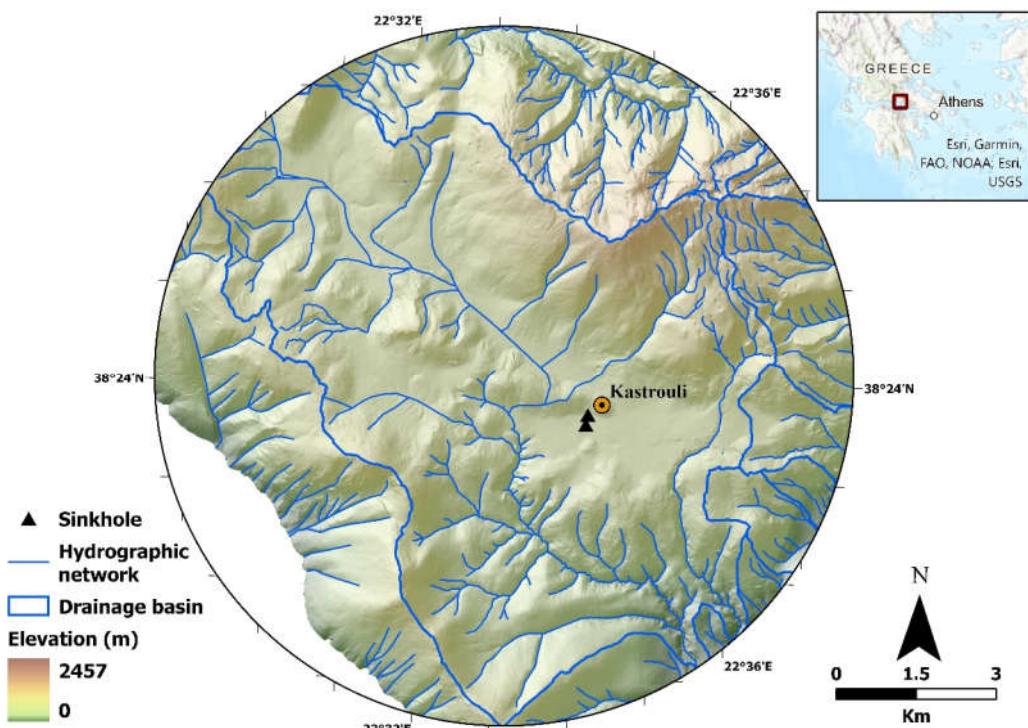


Figure 15. The well-developed hydrographic system of the wider Kastrouli area.

We believe that the drained area confines are most probably at the boundary encircled by a slope of less than 2 degrees ($\leq 3.49\%$) (less than 0.1 Km^2), whereas the two sinks' positions are relevant and close to the flooded area, where streams and torrents flow downhill and drainage is manageable (Figure 15).

Regarding ERT1, in the first 6 m, there are conductive, loose, clay materials, which are perhaps eroded materials from limestone (Figure 6). At the 60th meter along the topography, the limestone plunges to a depth of about 35 m. The geological map does not provide any fault indication (as a rift valley) or any bauxite ore body that could explain this image. The basin starts somewhere at about the 95th meter and ends at about 180 m, whereas it seems to reach a depth of 40 m, making the size of this highly conductive layer about 100 m by 30 m. As noted above, in the first 5–6 m, there are conductive materials, while below this formation, there is an antistatic layer of thickness of about 10–20 m. Further down, a relatively conductive formation appears, which may reflect an aquifer.

The existence of the sinkhole may be related to this layer, but our measurements are few, and a (planned) borehole will give more information. There is a sinking in the whole area, but regarding the sinkholes, we note with confidence that the sinks are located at a

slightly higher altitude than the basin. This is likely to be affected by the very existence of the zone in which conductive materials accumulate.

In the second section of ERT2 (Figures 6 and 7), the (same) basin is, again, clearly seen, which seems to reach a depth of about 40 m as also noted for ERT1. The basin therefore seems to start from the 260th meter and reaches up to the 340–350th meters along the tomography or about 100 m in length. As in ERT1 and here in the first few meters, we see the conductive material, while deeper, the existence of an antistatic aquifer is most probable.

The ERT and GIS-DEM data sway one's opinion to assume the presence of a cave in that area. That is, the rainwater found a way to dissolve the limestone perhaps together with the existence of a fault. This cave may have collapsed due to the action of a seismic fault, forming the basin and the accumulated deposits.

However, this hypothesis is to be tested if future research verifies the existence of a rift, perhaps conducting a borehole analysis of sediments. However, to date, such information has not been provided by the geological mapping of the area.

5. Conclusions

The set objectives of the present investigation were fulfilled. The sporadic flooding of the Meteles plain that occurs nowadays during winter in the vicinity of the Kastrouli prehistoric settlement (14th to 11th c. BCE) and the presence of two old sinks apparently engineered to lead seepage water into a natural aquifer present in the limestone bedrock were explained. The results of the combined ERT and GIS-DEM geophysical techniques confirmed these observations, indicating the alleged ancient hydraulic works in the area as having been a small lake in the past that developed into a marsh. The surficial entrance to the sinkholes implies that a marsh developed during the last 3500 years or so. The studied area close to the Kastrouli Mycenaean settlement, which seems to have been re-inhabited at later times, contains a basin with a total length close to 100 m in width and a depth somewhere between 40 and 50 m. It is a small basin with two sinks near it, which drain the water. These natural crevices were reworked by ancient inhabitants and may have continued to last centuries to aid the safe drainage of flooding. In fact, the flooded area and/or the formation of a marsh or swamp, perhaps a small ancient lake, was estimated with DEM and GIS sloping to be around 0.1 km², and these two sinkholes were found using ERT, as well as low resistivity values in that part of the bedrock. Future work includes boreholing and the study of the acquired sedimentary cores for dating formation, the origin of the sediments, and a palaeoecological reconstruction of the area.

Author Contributions: Conceptualization, I.L.; methodology, I.L., G.N.T., and N.E.; software, N.E., E.F., A.S., M.T., and P.L.; investigation, I.L., G.N.T., N.E., A.S., E.F., T.R., and N.D.; writing—original draft preparation, I.L.; resources, E.F., A.S., N.E., M.T., P.L., and T.R.; writing—review and editing, I.L., N.E., and G.N.T.; visualization, I.L., N.E., G.N.T., A.S., E.F., and M.T.; supervision, I.L., G.N.T., and N.E. All authors have read and agreed to the published version of the manuscript.

Funding: This research received no external funding.

Institutional Review Board Statement: Not applicable.

Informed Consent Statement: Not applicable.

Conflicts of Interest: The authors declare no conflicts of interest.

References

1. Lisetskii, F.N.; Stolba, V.F.; Pichura, V.I. Late-Holocene palaeoenvironments of Southern Crimea: Soils, soil-climate relationship and human impact. *Holocene* **2017**, *27*, 1859–1875. <https://doi.org/10.1177/0959683617708448>.
2. Hassan, F.A. Holocene lakes and prehistoric settlements of the Western Fayum, Egypt. *J. Archaeol. Sci.* **1986**, *13*, 483–501. [https://doi.org/10.1016/0305-4403\(86\)90018-X](https://doi.org/10.1016/0305-4403(86)90018-X).
3. Mamassis, N.; Moustakas, S.; Zarkadoulas, N. The operation of ancient reclamation works at Lake Copais in Greece. *Water Hist.* **2015**, *7*, 271–287. <https://doi.org/10.1007/s12685-015-0126-x>.

4. Koutsoyiannis, D.; Angelakis, A. Ancient Greece: Agricultural Hydraulic Works. In *Encyclopedia of Water Science*; Trimble, S.W., Ed.; CRC Press: Boca Raton, FL, USA, 2007; pp. 24–27.
5. Viollet, P.-L. *Water Engineering in Ancient Civilizations: 5000 Years of History*; CRC Press: Boca Raton, FL, USA, 2007; ISBN 9789078046059.
6. Kountouri, E.; Petrochilos, N.; Liaros, N.; Oikonomou, V.; Koutsoyiannis, D.; Mamassis, N.; Zarkadoulas, N.; Vött, A.; Hadler, H.; Henning, P.; et al. The Mycenaean drainage works of north Kopais, Greece: A new project incorporating surface surveys, geophysical research and excavation. *Water Supply* **2013**, *13*, 710–718. <https://doi.org/10.2166/WS.2013.110>.
7. Kolding, J.; Van Zwieten, P.A.M.; Martín, F.; Poulaïn, F. *Freshwater Small Pelagic Fish and Their Fisheries in Major African Lakes and Reservoirs in Relation to Food Security and Nutrition*; Food and agriculture organization of the United Nations, FAO Fisheries and Aquaculture Technical Paper No. 642: Rome, Italy, 2019.
8. Wilke, T.; Wagner, B.; Van Bocxlaer, B.; Albrecht, C.; Ariztegui, D.; Delicado, D.; Francke, A.; Harzhauser, M.; Hauffe, T.; Holtvoeth, J.; et al. Scientific drilling projects in ancient lakes: Integrating geological and biological histories. *Glob. Planet. Change* **2016**, *143*, 118–151. <https://doi.org/10.1016/J.GLOPLACHA.2016.05.005>.
9. O’Sullivan, A. Interpreting the Archaeology of Late Bronze Age Lake Settlements. *J. Irish Archaeol.* **1997**, *8*, 115–121.
10. Hoppenbrock, J.; Bücker, M.; Gallistl, J.; Flores Orozco, A.; de la Paz, C.P.; García García, C.E.; Razo Pérez, J.A.; Buckel, J.; Pérez, L. Evaluation of Lake Sediment Thickness from Water-Borne Electrical Resistivity Tomography Data. *Sensors* **2021**, *21*, 8053. <https://doi.org/10.3390/s21238053>.
11. Valipour, M.; Krasilnikoff, J.; Yannopoulos, S.; Kumar, R.; Deng, J.; Roccaro, P.; Mays, L.; Grismer, M.E.; Angelakis, A.N. The Evolution of Agricultural Drainage from the Earliest Times to the Present. *Sustainability* **2020**, *12*, 416. <https://doi.org/10.3390/su12010416>.
12. Kollyropoulos, K.; Antoniou, G.P.; Kalavrouziotis, I.K.; Krasilnikoff, J.A.; Koutsoyiannis, D.; Angelakis, A.N. Hydraulic Characteristics of the Drainage Systems of Ancient Hellenic Theatres: Case Study of the Theatre of Dionysus and Its Implications. *J. Irrig. Drain. Eng.* **2015**, *141*, 04015018. [https://doi.org/10.1061/\(ASCE\)IR.1943-4774.0000906](https://doi.org/10.1061/(ASCE)IR.1943-4774.0000906).
13. De Feo, G.; Mays, L.W.; Angelakis, A.N. Water and Wastewater Management Technologies in the Ancient Greek and Roman Civilizations. *Treatise Water Sci.* **2011**, *4*, 3–22. <https://doi.org/10.1016/B978-0-444-53199-5.00071-3>.
14. Mays, L.W. *Ancient Water Technologies*; Springer: Dordrecht, The Netherlands, 2010; ISBN 9789048186310.
15. Farinetti, E. *A GIS-Based Study for the Reconstruction and Interpretation of the Archaeological Datasets of Ancient Boeotia*; Archaeopress: Oxford, UK, 2011.
16. Sideris, A.; Liritzis, I.; Liss, B.; Howland, M.D.; Levy, T.E. At-risk cultural heritage: New excavations and finds from the Mycenaean site of Kastrouli, Phokis, Greece. *Mediterr. Archaeol. Archaeom.* **2017**, *17*, 271–285. <https://doi.org/10.5281/zenodo.163772>.
17. Liritzis, I.; Polymeris, G.S.; Vafiadou, A.; Sideris, A.; Levy, T.E. Luminescence dating of stone wall, tomb and ceramics of Kastrouli (Phokis, Greece) Late Helladic settlement: Case study. *J. Cult. Herit.* **2019**, *35*, 76–85. <https://doi.org/10.1016/J.CULHER.2018.07.009>.
18. Liritzis, I.; Xanthopoulou, V.; Palamara, E.; Papageorgiou, I.; Iliopoulos, I.; Zacharias, N.; Vafiadou, A.; Karydas, A.G. Characterization and provenance of ceramic artifacts and local clays from Late Mycenaean Kastrouli (Greece) by means of p-XRF screening and statistical analysis. *J. Cult. Herit.* **2020**, *46*, 61–81. <https://doi.org/10.1016/J.CULHER.2020.06.004>.
19. Xanthopoulou, V.; Iliopoulos, I.; Liritzis, I. Mineralogical and Microstructure Analysis for Characterization and Provenance of Ceramic Artifacts from Late Helladic Kastrouli Settlement, Delphi (Central Greece). *Geosciences* **2021**, *11*, 36. <https://doi.org/10.3390/geosciences11010036>.
20. Levy, T.E.; Sideris, T.; Howland, M.; Liss, B.; Tsokas, G.; Stambolidis, A.; Fikos, E.; Vargemezis, G.; Tsourlos, P.; Georgopoulos, A.; et al. At-Risk World Heritage, Cyber, and Marine Archaeology: The Kastrouli–Antikyra Bay Land and Sea Project, Phokis, Greece. In *Cyber-Archaeology and Grand Narratives: Digital Technology and Deep-Time Perspectives on Culture Change in the Middle East*; Levy, T.E., Jones, I.W.N., Eds.; Springer International Publishing: Cham, Switzerland, 2018; pp. 143–234, ISBN 978-3-319-65693-9.
21. Cantu, K.; Norris, R.; Papatheodorou, G.; Liritzis, I.; Langgut, D.; Geraga, M.; Levy, T. Anthropogenic Erosion from Hellenistic to Recent Times in the Northern Gulf of Corinth, Greece. In *Mediterranean Resilience Collapse and Adaptation in Antique Maritime Societies*; Yasur-Landau, A., Gambash, G., Levy, E., Eds.; Equinox eBooks Publishing: Sheffield, UK, 2022.
22. Liritzis, I. Kastrouli fortified settlement (Desfina, Phokis, Greece): A chronicle of research. *Sci. Cult.* **2021**, *7*, 17–32. <https://doi.org/10.5281/zenodo.4465472>.
23. Koh, A.J.; Birney, K.J.; Roy, I.M.; Liritzis, I. The mycenaean citadel and environs of desfina-kastrouli: A transdisciplinary approach to southern phokis. *Mediterr. Archaeol. Archaeom.* **2020**, *20*, 47–73. <https://doi.org/10.5281/zenodo.3930420>.
24. Tsourlos, P. *Modeling, Interpretation and Inversion of Multielectrode Resistivity Survey Data*; University of York: York, UK, 1995.
25. Tagg, C. *Earth Resistances*; Pitman Publishing Company: New York, NY, USA, 1964.
26. McNeill, J. *Electromagnetic Terrain Conductivity Measurement at Low Induction Numbers*; Canada, 1980.
27. Schlumberger, C. *Etude sur la Prospection Electrique du Sous-sol*; Gauthier-Villars: Paris, France, 1920.
28. Kim, J. DC2DPro-2D Interpretation System of DC Resistivity Tomography. User’s Manual and Theory, KIGAM, Korea Institute of Geoscience and Mineral Resources: Daejeon, South Korea 2009.
29. Coveney, S.; Stewart Fotheringham, A.; Charlton, M.; McCarthy, T. Dual-scale validation of a medium-resolution coastal DEM with terrestrial LiDAR DSM and GPS. *Comput. Geosci.* **2010**, *36*, 489–499. <https://doi.org/10.1016/J.CAGEO.2009.10.003>.

30. Schmid, K.A.; Hadley, B.C.; Wijekoon, N. Vertical Accuracy and Use of Topographic LIDAR Data in Coastal Marshes. *J. Coast. Res.* **2011**, *27*, 116–132. <https://doi.org/10.2112/JCOASTRES-D-10-00188.1>.
31. Manfreda, S.; McCabe, M.F.; Miller, P.E.; Lucas, R.; Pajuelo Madrigal, V.; Mallinis, G.; Ben Dor, E.; Helman, D.; Estes, L.; Ciraolo, G.; et al. On the Use of Unmanned Aerial Systems for Environmental Monitoring. *Remote Sens.* **2018**, *10*, 641. <https://doi.org/10.3390/rs10040641>.
32. Ford, D.; Williams, P. Karst Hydrogeology. In *Karst Hydrogeology and Geomorphology*; John Wiley & Sons, Ltd.: Hoboken, NJ, USA, 2007; pp. 103–144, ISBN 9781118684986.
33. Ford, D.; Williams, P. Analysis of Karst Drainage Systems. In *Karst Hydrogeology and Geomorphology*; John Wiley & Sons, Ltd.: Hoboken, NJ, USA, 2007; pp. 145–208 ISBN 9781118684986.
34. Marinos, P.; Rondoyanni, T. The Archaeological Site of Delphi, Greece: A Site Vulnerable to Earthquakes, Rockfalls and Landslides. In *Landslides: Risk Analysis and Sustainable Disaster Management*; Sassa, K., Fukuoka, H., Wang, F., Wang, G., Eds.; Springer: Berlin/Heidelberg, Germany, 2005; pp. 241–249, ISBN 978-3-540-28680-6.
35. Celet, P. Quelques aspects de l’hydrogeologie des regions calcaires meridionales du Parnasse-Helicon (Grece). *Ann Sci. Pays Hell.* **1971**, *3*, 13–16.